

Tracking Trajectory Control of Dual-eyes Visual-based Underwater Vehicle*

Naoki Mukada¹, Kenta Yonemori¹, Myo Myint¹, Khin Nwe Lwin¹, Akira Yanou² and Mamoru Minami¹

Abstract—Nowadays, a variety of robots have been studied and developed for undersea exploration. The purpose of undersea exploration is to retrieve resources such as methane hydrate rare metal from bottom of sea. The ability for underwater vehicle to recharge batteries automatically in the sea is vital function so that the vehicle achieves the required tasks with long duration time, raising next technical problems of how the guide the vehicle to the recharging station and how to avert surrounding hazardous environment.

One approach to solve the problem is to control the vehicle's trajectory by using visual information. This paper proposes a method to guide a vehicle to desired trajectory with dual-eye visual feedback, which utilizes inverse Jacobian matrix to generate desired trajectory in the underwater space. The experimental results show that the proposed control scheme is effective to have the vehicle follow the desired trajectories.

I. INTRODUCTION

Nowadays, underwater robots are being used in various scenes, for example, recovery of dead fishes that are sank to the bottom of the water in the fish farming industry, damage investigation of the fishing port that was affected by the earthquake, inspection of dam walls and equipment inspection at the hydroelectric power plant. Among them, in harsh environments that cannot be entered by the human such as seabed survey with depth of several hundred to several thousand meters, the use of these robots is greatly expected.

However, when carrying out seabed surveys, seabed mapping, biological surveys, etc, there is a need for a long period of time navigation of the underwater robot. When using a Remotely Operated Vehicle (ROV) that is intended to be powered by a wire from the sea, there are various problems such as adverse effect on the control of underwater robot due to a disturbance of the tension of the cable, limitation for deep operation, etc. Even though AUVs equipped with a battery can eliminate this issue, battery charging for long period of seabed survey become a problem because current battery capacity are on the order of a few hours. Therefore, to realize a long period of operation in water, it is an ideal case for the underwater vehicle to perform charging automatically in the underwater station that is set up with power feeding equipment. Therefore, studies on the guidance and control system to perform docking function for underwater charging automatically has been actively carried out. We have been

doing underwater vehicle research developing real-time 3D position and orientation recognition of 3D marker using video images from dual-eye camera. We named our proposed system as Three Dimensional Move on Sensing (3D-MoS). In previous work [1], real time pose tracking was confirmed even through there were air bubble disturbance in front of cameras. We also implemented docking operation for underwater battery recharging application [2]. The robustness of the system under dynamic light environment was verified in [3]. It should be noted that the robot performed docking automatically by means of visual servoing in which images acquired from dual-eye camera are used for recognition of docking station. We conducted not only docking experiments in the pool but also in the sea of Wakayama Prefecture successfully [4]. However, various obstacles may present in the bottom of the sea while an underwater robot approaches to a docking station. Therefore, it is necessary to operate the underwater vehicle to approach the docking station avoiding the obstacles. Installation of docking station with powered equipment in the area where there is no obstacles and avoiding obstacles in advance is realistic option. However, when we expand the research of visual servoing using 3D-MoS in future for natural environment with rock and renovations, technology that makes vehicle approach the target automatically while avoiding the obstacles has become essential. Most researches on robot control have assumption of exact kinematics and Jacobian matrix of manipulator [5]-[6]. However, this kind of approach does not work for the underwater vehicle with uncertain kinematics and dynamics especially while interacting with unknown environment. There are some studies on approximate Jacobian feedback control of robots [7]-[8]. However, they have not been experimentally verified and work space is only for manipulator. Therefore, in proposed method, the Jacobian matrix that indicates relationship between generated thrust voltage and underwater robot performance was experimentally measured. In this paper, we propose and report performance of a control method to follow the target trajectory by using inverse Jacobian matrix that is experimentally measured to indicate the relationship between generated thrust voltage and underwater robot performance.

II. THE NEED FOR TRAJECTORY TRACKING CONTROL

The docking operation process simulated for underwater battery charging is shown in Fig. 1. Signal source (A) such as acoustic sensor installed in docking station propagates signal to guidance the vehicle (B) to approach the station for charging following the track (1). When there is a rock (X) on

*This work was not supported by any organization

¹Graduate School of Nature Science and Technology, Okayama University, 3-1-1 Tushima-naka, Kita-ku, Okayama, 700-8530, Japan minami-m@cc.okayama-u.ac.jp

²Department of Radiology Technology, Kawasaki College of Allied of Allied Health Professions, Kurashiki, Okayama, 701-0194, Japan yanou-a@mw.kawasaki-m.ac.jp

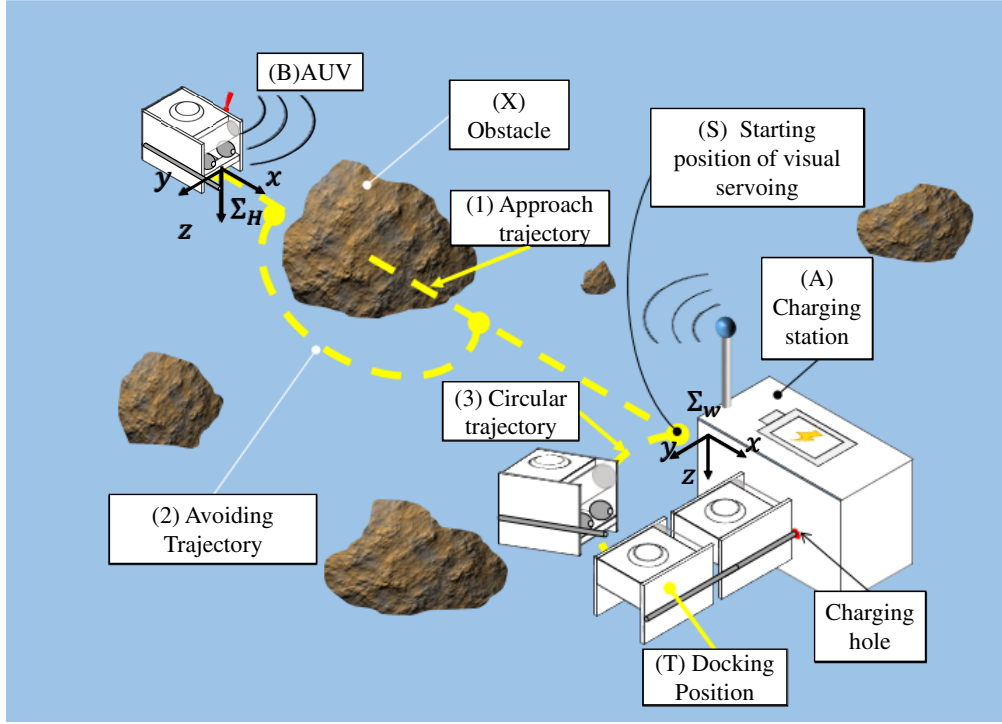


Fig. 1. Simulated environment

the track, AUV has to follow the trajectory (2) in horizontal direction to avoid the rock and return to the initial track at the point (R). Even though the avoidance way is assumed as shown in Fig. 1, the trajectory to avoid the rock can also be in vertical direction. Then, the vehicle moves to the point (S) where the vehicle can navigate itself using visual servoing. From (S) point towards the point (T), the vehicle has to move on a circular track (3) leading to the (T) point. The fitting process by visual servoing is then completed. The above all scenario is assumed one. In this way, it is assumed that there are various obstacles, such as rocks in the ocean floor while the underwater robot approaching to the target. Therefore, to generate a trajectory to avoid obstacles when moving to the power supply equipment is necessary for controlling the vehicle for application such as recharging. It is also convenience for fitting process when the vehicle is not facing directly to the docking hole for recharging power. In this case, to generate a trajectory including the position and orientation information is necessary to fit to the fitting hole by using the trajectory tracking control. Therefore, in this study, we propose a new method for inducing control the AUV on the position and posture trajectory of the goal while performing a visual servo using the 3D-MoS.

III. TRAJECTORY TRACKING CONTROL METHOD

A. Control Method

We considered that cable shape is constant in small area in which ROV moves. Jacobi matrix, \mathbf{J} does not depend on the ROV's states, it relates to how the tether cable affects to the

ROV. The velocity vector is defined as $\dot{\mathbf{r}}[\dot{x}, \dot{y}, \dot{z}, \dot{\theta}]$ (m/s) with respect to Σ_w which was set to target object as shown in Fig. 1. (θ is the angle around the z axis of Σ_H , and angles around other axis are neglected to be controlled because these are stabilized naturally by the structure of the vehicle and less effective to controlling vehicle.) Input voltage to an amplifier of thrust motor is shown as \mathbf{v} (V), It's possible to show a relation between \mathbf{v} and $\dot{\mathbf{r}}$ as (1) using Jacobi matrix.

$$\dot{\mathbf{r}} = \mathbf{J}\mathbf{v} \quad (1)$$

where

$$\mathbf{J} = \begin{bmatrix} \frac{\partial \dot{x}}{\partial v_1} & \frac{\partial \dot{x}}{\partial v_2} & \frac{\partial \dot{x}}{\partial v_3} & \frac{\partial \dot{x}}{\partial v_4} \\ \frac{\partial \dot{y}}{\partial v_1} & \frac{\partial \dot{y}}{\partial v_2} & \frac{\partial \dot{y}}{\partial v_3} & \frac{\partial \dot{y}}{\partial v_4} \\ \frac{\partial \dot{z}}{\partial v_1} & \frac{\partial \dot{z}}{\partial v_2} & \frac{\partial \dot{z}}{\partial v_3} & \frac{\partial \dot{z}}{\partial v_4} \\ \frac{\partial \dot{\epsilon}_3}{\partial v_1} & \frac{\partial \dot{\epsilon}_3}{\partial v_2} & \frac{\partial \dot{\epsilon}_3}{\partial v_3} & \frac{\partial \dot{\epsilon}_3}{\partial v_4} \end{bmatrix} \quad (2)$$

Feed forward control has been firstly designed as (3)

$$\begin{aligned} \mathbf{v} &= \mathbf{J}^{-1} \dot{\mathbf{r}}_d \\ &= \mathbf{J}^{-1} \mathbf{K}_P (\mathbf{r}_d - \mathbf{r}) \end{aligned} \quad (3)$$

where, proportional gain, the target location, target speed and present location are defined as \mathbf{K}_P (diagonal matrices of 4×4) (1/s), \mathbf{r}_d (m), $\dot{\mathbf{r}}_d$ (m/s), \mathbf{r} (m).

However, when $(\mathbf{r}_d - \mathbf{r})$ is equal to 0 in case of using only feedback control of the position, $\mathbf{v} = 0$ is output. As a result, there will be steady state error neglecting the

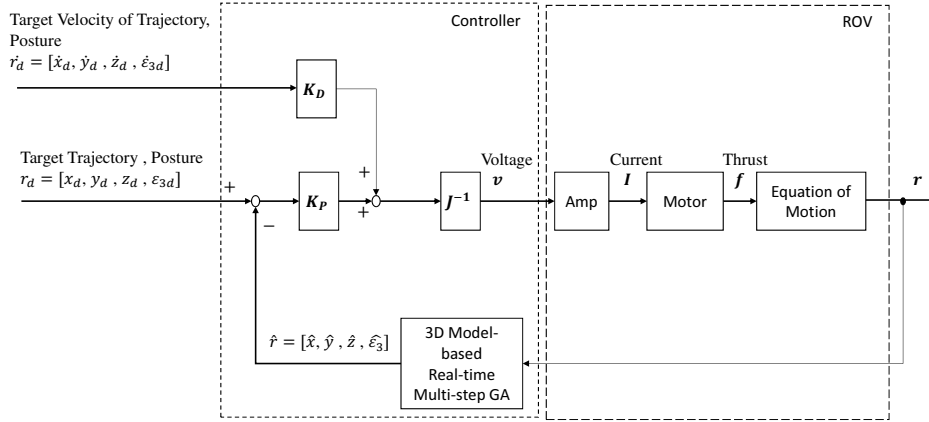


Fig. 2. Visual servoing system using feedforward and feedback control Three Dimensional Move on Sensing(3D-MoS) including Multi-step GA

velocity of target trajectory because of delay in controlling. Therefore, the trajectory tracking control method combining feed forward and feedback is used in this work as shown in (4). Feed forward input with respect to the velocity of the target trajectory is set to improve trajectory tracking control performance.

A gain for feed forward input is defined as K_D . Position and orientation r is written as \hat{r} . \hat{r} is estimated vector by using Real-time Multi-step GA[9], which makes GA evolve more than one time for dynamic images. Fig. 2 shows the block diagram of the control law of (3) together with ROV. The left block shown as a dotted line is a controller, and a right broken line indicates ROV. Real time 3D recognition was utilized using Real-time Multi-step GA in which gene evaluation is performed as much as possible for optimization to find estimated pose after a RGB image from dual cameras was input every 33 ms. PC (Processor: Intel(R) Core(TM) i7-4790 CPU @ 3.60 (GHz), RAM: 8.00 (GB)) is used to complete real time pose estimation and 3D motion control as software implementation. Computing time is about 3.6 (ms) per 1 generation, and 9 times of evolution is possible.

$$v = J^{-1}(K_P(r_d - \hat{r}) + K_D \dot{r}_d) \quad (4)$$

IV. PREPARATION OF EXPERIMENT

A. Underwater vehicle

Hovering type underwater vehicle (manufactured by Kowa cooperation) is used as a test bed as shown in Fig.3. Two fixed cameras installed at the front of the vehicle. In thruster unit, four thrusters with maximum thrust force of 4.9 each are controlled to move the vehicle along desired path. The vehicle can dive up to 50 (m) and two LED light sources are also installed on the vehicle.

B. Experiment Environment

The experimental environment of ROV is shown in Fig. 4. The pool (length \times width \times height, 2 (m) \times 3 (m) \times 0.75 (m)) filled with water was used as an experimental tank. We set up strings over the pool with interval of 500 (mm)

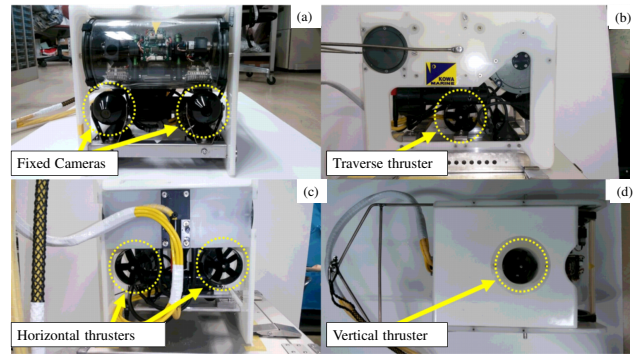


Fig. 3. Overview of ROV (a)Front view (b)Side view (c)Back view (d)Top view

as shown in Fig. 4. We analyzed a movement trajectory of ROV by using strings interval from the movie which we took during experiments. We analyzed ROV movement which was controlled by input from a PC. Signal exchange between the PC and ROV was done through tether cable (200 (m)). A relation between input voltage and thrust is nonlinear function including deadzone, but the function was converted to linear relation by software implementation.

C. Jacobi Matrix Estimation Method

We took a movie of movement trajectory in each axis direction of (x, y, z, ϵ_3) when a voltage is input to one of axis of thrust, using a fixed camera above pool.

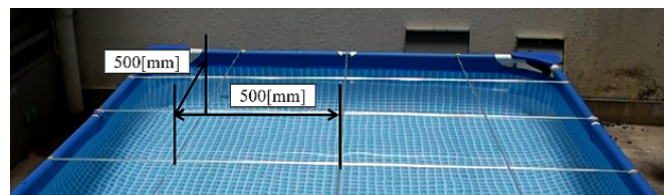


Fig. 4. Experimental environment

The amount of movement in each axis was measured from the movie using interval of strings and the velocity in each axis was calculated. Measurement start time was defined only when the velocity of ROV became steady velocity. The velocity of ROV became steady speed in about 3 seconds.

An example of measuring in the x axis direction is indicated in (5). In case of measurement, input voltage to ROV is adjusted to make a thrust occur linearly in +1.2 (V) from -1.2 (V). A voltage that makes ROV stop is 0 (V). (5) shows Jacobi matrix with ingredients J_{11} - J_{44} are ingredients. -1.2 (V) is input to thruster for x axial movement and 0 (V) is input to the other thruster. As a result, ROV moves forward. We measured the influence on the movement in y axis direction during this movement, and updated each ingredient using measured value. The measurement state of the velocity ingredient in each axis are indicated in Fig. 5-8. Here, subfigure (a) is measurement at start time, (b) is measurement at middle time, and (c) is measurement at end time.

$$\begin{bmatrix} \dot{x} \\ \dot{y} \\ \dot{z} \\ \dot{\epsilon}_3 \end{bmatrix} = \begin{bmatrix} J_{11} & J_{12} & J_{13} & J_{14} \\ J_{21} & J_{22} & J_{23} & J_{24} \\ J_{31} & J_{32} & J_{33} & J_{34} \\ J_{41} & J_{42} & J_{43} & J_{44} \end{bmatrix} \begin{bmatrix} -1.2 \\ 0 \\ 0 \\ 0 \end{bmatrix} \quad (5)$$

D. Analysis Experimental Result

A result of measurement of amount of movement in each axis is indicated in table I. It could be confirmed that an influence about the velocity to the other axis direction is also caused when individual input is applied to each axis. The velocity of the biggest thrust was calculated and relation between the velocity and the voltage was calculated by using calculated velocity. The result of relation is indicated in table II. Jacobi matrix is derived from these calculation. Obtained Jacobi matrix is shown in (6).

$$\mathbf{J} = \begin{bmatrix} 0.1483 & 0.0030 & 0 & 0 \\ 0.0148 & 0.0303 & 0 & 0.0442 \\ 0 & 0 & -0.0690 & 0 \\ 0 & 0 & 0.0002 & 0.0020 \end{bmatrix} \quad (6)$$

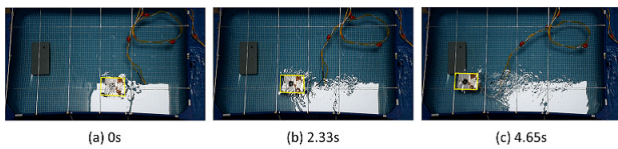


Fig. 5. Measurement state of X axis direction

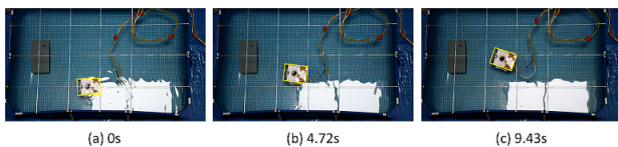


Fig. 6. Measurement state of Y axis direction

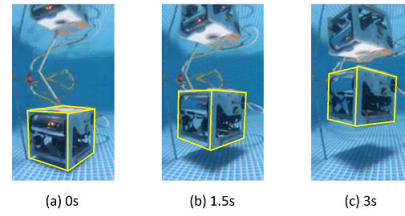


Fig. 7. Measurement state of Z axis direction

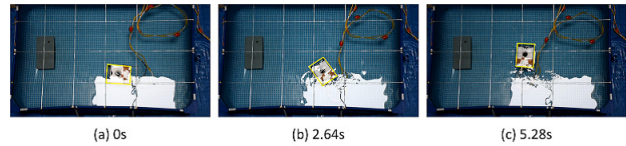


Fig. 8. Measurement state of around Z axis

TABLE I
MOVING DISPLACEMENT IN EACH AXIS

		Voltage Inputted Axis			
		x	y	z	ϵ_3
Moving displacement in each axis	x [cm]	100	5	0	0
	y [cm]	10	50	0	35
	z [cm]	0	0	-30	0
	ϵ_3 [deg]	0	2	5	90
Measuring Time	[s]	4.65	9.43	3	5.28

TABLE II
VELOCITY PER VOLTAGE IN EACH AXIS

		Voltage Inputted Axis			
		x	y	z	ϵ_3
Slope in each axis	x [m/s]	0.1483	0.0030	0	0
	y [m/s]	0.0148	0.0303	0	0.0442
	z [m/s]	0	0	-0.0690	0
	ϵ_3 [rad/s]	0	0	0.0002	0.0020

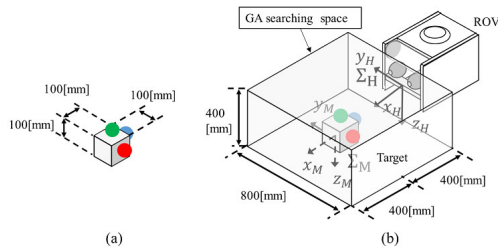


Fig. 9. (a)3D marker and (b)Underwater target and GA search space

TABLE III
PARAMETERS FOR GA

Target variables calculated by GA	Positions (x [mm], y [mm], z [mm]), Posture (ϵ_3 [deg])
Number of genes	60
Length of genes	72 bit
Selection rate	0.6
Crossover	two-point crossover
Mutation rate	0.1
Search area (as centering the target in this area) [mm]	$\{x,y,z\} = \{\pm 400, \pm 200, \pm 400\}$
Control period [ms]	33
Number of generation evolution in the control period	9

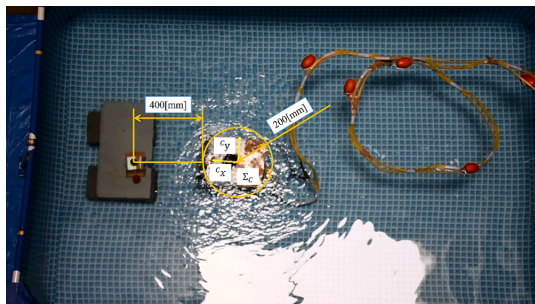


Fig. 10. Desired trajectory in X and Y direction

V. TRAJECTORY TRACKING CONTROL EXPERIMENT USING CIRCULAR TRAJECTORY

The underwater vehicle, the experimental environment and the condition to conduct a trajectory tracking control experiment are same as the previous work[2]. Searching space of 3D marker and GA is shown in Fig. 9 and a parameter of GA is shown to table III. The initial position which begins trajectory tracking control is shown in (7). Therefore, the initial position is defined as coordinate system Σ_C and a trajectory is generated with respect to this coordinate system. The target trajectory used for tracking is shown in (8) and a target trajectory velocity is indicated in (9). A trajectory including the position relationship with the target object is indicated on Fig. 10. A feedback gain $K_{P\epsilon_3}$ (1/s) for rotation is 5.0, feedback gains $[K_{Px}$ (1/s), K_{Py} (1/s), K_{Pz} (1/s)] for movement were given by three values for each

cycle as follow $[0.15,0.15,0.05],[0.3,0.3,0.1],[0.6,0.6,0.2]$ in each cycle. Total of 9 times of experiment was conducted.

$$\begin{cases} x = {}^H x_M = 400 \\ y = {}^H y_M = 0 \\ z = {}^H z_M = -40 \\ \epsilon_3 = {}^H \epsilon_{3M} = 0 \end{cases} \quad (7)$$

$$\begin{cases} {}^C x(t) = -200 \cos\left(\frac{2\pi}{T}t\right) + 400 \\ {}^C y(t) = 200 \sin\left(\frac{2\pi}{T}t\right) \end{cases} \quad (8)$$

$$\begin{cases} {}^C \dot{x}(t) = \frac{400\pi}{T} \sin\left(\frac{2\pi}{T}t\right) \\ {}^C \dot{y}(t) = \frac{400\pi}{T} \cos\left(\frac{2\pi}{T}t\right) \end{cases} \quad (9)$$

VI. RESULT AND DISCUSSION

A. Trajectory Tracking Control Result

The averaged movement of the vehicle was shown in Fig. 11. All results indicate data seen from Σ_C , and the calculation of averaged movement is based on 30 data (the interval of each data is 33 (ms).) where the averaged movement from data was calculated every 1 second. Fig. 11 shows that the tracking performance is improved when the larger feedback gain was given in the each cycle. According to experimental result, tracking performance is smooth with the longer duration of desired cycle trajectory.

B. Trajectory Tracking Control Performance

An experimental result of trajectory tracking control performance in time domain in y and x axis direction is shown in Fig. 12. The trajectory tracking control start time is defined as 0 (s) and the amount of movement in y and x axis direction in the condition of cycle 23 (s) is shown in (a) and (b) respectively. Similarly, the amount of movement of vehicle in y and x axis direction in the condition of cycle 47 (s) is shown in (c) and (d), and 70 (s) is shown in (e) and (f). When we consider about the amount of movement in the x axis direction, there is a phase error in following a target trajectory. However, we can confirm that ROV approximately follows the trajectory in each cycle. When movement in the y axis direction was analysed, a significant phase error occurred in the case of shorter duty cycle of 23 (s) error has . In particular, when the smallest gain was used, an actual trajectory in the y axis direction is an anti-phase to a target trajectory, and a control result becomes unstable. In that condition, ROV could not conduct trajectory tracking control well as shown in Fig. 11(a). Regarding different behaviour in x and y direction, it seems that number of used thrusters influences on control performance. While two thrusters are used for the movement in x axis direction, only one thruster is used for y axis direction. We developed our method to measure and analyse motion control of ROV experimentally for estimation of Jacobi matrix. According to experimental result it was confirmed that trajectory tracking performance can be improved depending on the precision of the estimated Jacobi matrix.

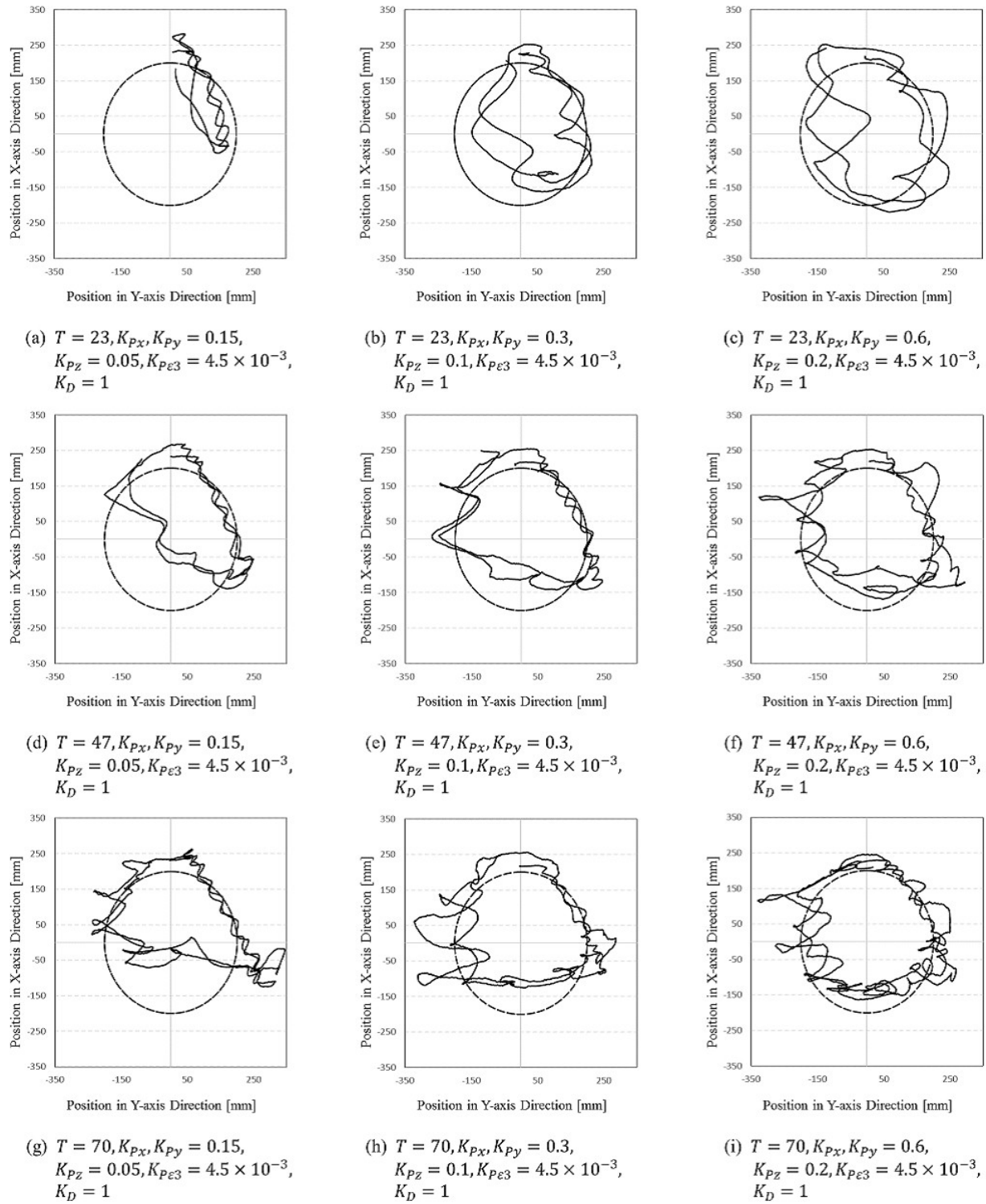
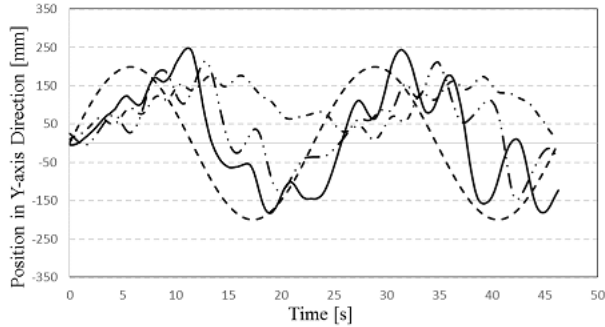
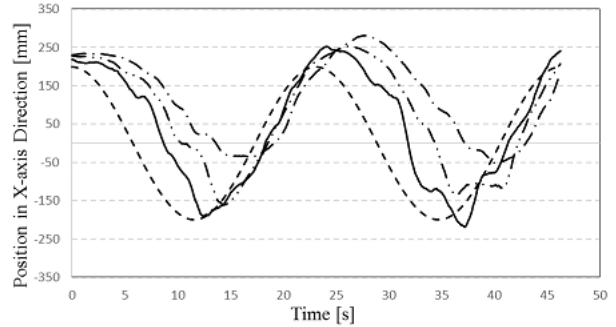


Fig. 11. Moving Average deviations of position in X axis and Y axis direction in each condition

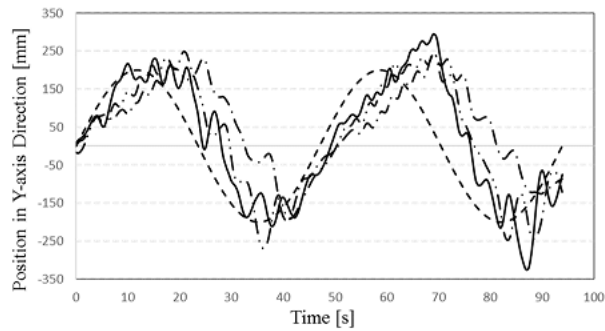
- Desired trajectory
- - - Actual trajectory ($K_{Px}, K_{Py} = 0.15, K_{Pz} = 0.05, K_{P\epsilon 3} = 4.5 \times 10^{-3}, K_D = 1$)
- · - Actual trajectory ($K_{Px}, K_{Py} = 0.3, K_{Pz} = 0.1, K_{P\epsilon 3} = 4.5 \times 10^{-3}, K_D = 1$)
- Actual trajectory ($K_{Px}, K_{Py} = 0.6, K_{Pz} = 0.4, K_{P\epsilon 3} = 4.5 \times 10^{-3}, K_D = 1$)



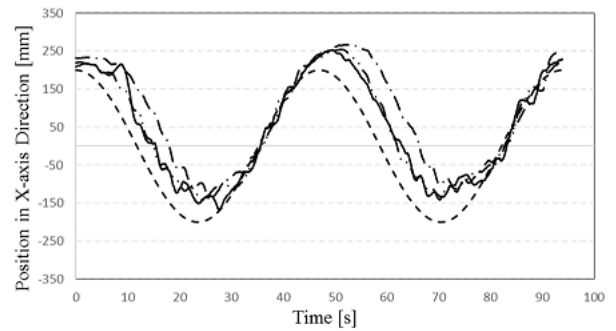
(a) Position in Y-axis direction at $T = 23$ s



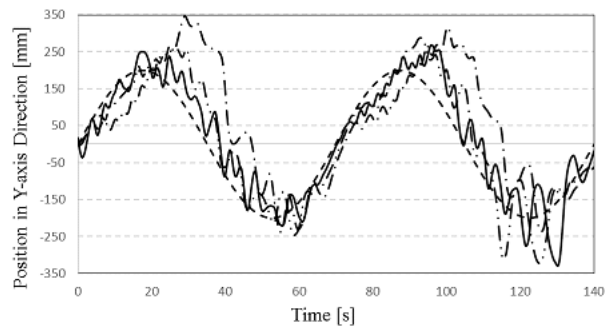
(b) Position in X-axis direction at $T = 23$ s



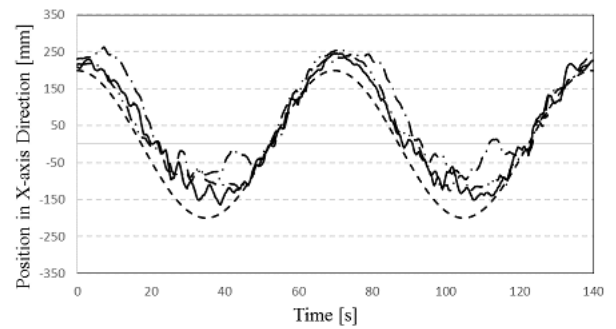
(c) Position in Y-axis direction at $T = 47$ s



(d) Position in X-axis direction at $T = 47$ s



(e) Position in Y-axis direction at $T = 70$ s



(f) Position in X-axis direction at $T = 70$ s

Fig. 12. Control result of position in X axis and Y axis direction in each period

VII. CONCLUSIONS

We have been developing ROV for avoidance behavior to obstacles and smooth movement to recharging point by means of trajectory tracking control. In this work, we conducted circular trajectory tracking control experiment using Jacobi matrix measured experimentally. As a result, We got the following conclusions.

(1) It was confirmed that ROV can be controlled by using estimated Jacobi matrix.

(2) Circular trajectory tracking control can be performed by controlling the vehicle using estimated Jacobi matrix in which movement of ROV in each axis direction is coupled to each other. Conducting experiment in real sea using proposed system is our future work for underwater battery recharging application.

A result of this report, we'll aim at further improvement of the trajectory tracking control performance.

REFERENCES

- [1] Myo Myint, Kenta YONEMORI, Akira YANOU, Shintaro ISHIYAMA and Mamoru MINAMI, Robustness of Visual-Servo against Air Bubble Disturbance of Underwater Vehicle System Using Three-Dimensional Marker and Dual-Eye Cameras, MTS/IEEE OCEANS, Washington, 18.Oct - 22.Oct, 2015
- [2] Akira , Y. Shota , O. Shintaro , I. and Mamoru , M, Autonomous docking control of visual-servo type underwater vehicle system aiming at underwater automatic charging, Transactions of the JSME, Vol. 81 (2015) No. 832 p. 15-00391.
- [3] Myo Myint, Kenta Yonemori, Akira Yanou, Khin Nwe Lwin, Mamoru Minami and Shintaro Ishiyama, Visual-based Deep Sea Docking Simulation of Underwater Vehicle Using Dual-eyes Cameras with Lighting Adaptation, MTS/IEEE OCEANS, Shanghai International Convention Center, April 10-13, 2016
- [4] NIHON KEIZAI SHINBUN, (2016/2/8) (in Japanese).
- [5] P. Tomei, Robust adaptive friction compensation for tracking control of robot manipulators, IEEE Trans, Automat. Contr., vol.45, pp 2164-2169, Nov.2000.
- [6] A. D. Luca, Feedforward/feedback laws for the control of flexible robots, in Proc. IEEE Conf. Robotics and Automation, San Francisco, CA, 2000, pp. 233-240.
- [7] C.C. Cheap, S. Kawamura, and S. Arimoto, Feedback control for robotic manipulators with uncertain kinematics and dynamics, in Proc. IEEE Int. Conf. Robotics and Automation, Leuven, Belgium, 1998, pp.3607-3612.
- [8] C.C. Cheah, S. Kawamura, S. Arimoto, and K. Lee, PID control for robotic manipulator with uncertain Jacobian matrix, in Proc. IEEE Int.Conf. Robotics and Automation, Detroit, MI, May 1999, pp. 494-499.
- [9] Myo Myint, Mamoru Minami, Kenta Yonemori, Khin Lwin, Akira Yanou, Dual-eyes Visual-based Sea Docking for Sea Bottom Battery Recharging, MTS/IEEE OCEANS' 16, September 19-23, 2016.